

UNCLASSIFIED

Defense Technical Information Center  
Compilation Part Notice

ADP010895

TITLE: The Origin of Complexity

DISTRIBUTION: Approved for public release, distribution unlimited

This paper is part of the following report:

TITLE: Paradigms of Complexity. Fractals and  
Structures in the Sciences

To order the complete compilation report, use: ADA392358

The component part is provided here to allow users access to individually authored sections of proceedings, annals, symposia, ect. However, the component should be considered within the context of the overall compilation report and not as a stand-alone technical report.

The following component part numbers comprise the compilation report:

ADP010895 thru ADP010929

UNCLASSIFIED

# THE ORIGIN OF COMPLEXITY

LEON O. CHUA

*Department of Electrical Engineering and Computer Sciences,  
University of California at Berkeley,  
Berkeley, CA 94720, USA  
E-mail: chua@eecs.berkeley.edu*

Nature abounds with complex *patterns* and *structures* emerging from *homogeneous media* operating far from thermodynamic equilibrium. Such phenomena, which are widely observed in both inanimate (non-biological) and biological media, can be modeled and studied via the CNN (Cellular Neural/Nonlinear Network) paradigm in an in-depth and unified way. Whether a homogeneous medium is capable of exhibiting complexity depends on whether the CNN *cells*, or its *couplings*, is *locally active* in a precise *mathematical* sense. This *local activity principle* is of universal generality and is responsible for all symmetry breaking phenomena observed in a great variety of non-equilibrium media ranging from the emergence of negative differential conductance in bulk semiconductor materials (e.g., Gallium Arsenide in Gunn Diodes) to the emergence of artificial life itself. The main result of this paper consists of a set of explicit *analytical conditions* for calculating the *parameter ranges necessary for the emergence* of a non-homogeneous static or dynamic pattern in a homogeneous medium operating under an influx of energy and/or matter. The resulting “complexity related” inequalities are applicable to all media, continuous or discrete, which have been mapped into a CNN paradigm.

*One of the most interesting aspects of the world is that it can be considered to be made up of patterns. A pattern is essentially an arrangement. It is characterized by the order of the elements of which it is made rather than by the intrinsic nature of these elements.*

*Norbert Wiener*

## 1 Introduction

How does the leopard get its spots? How does the zebra get its stripes? How does the fingerprint get its patterns? How does an ant colony manage to *self-organize* into an impressive pattern of activities when individual ants are known to be quite dumb? How does an initially mixed distribution of black and white population in a housing community manage to redistribute over time into segregated black and white neighborhoods with well-defined boundaries?

How does a bee sting at a finger tip trigger the propagation of an electrical impulse to the brain of a healthy person, and how does this distress signal fail to propagate in the nerves of patients suffering from multiple sclerosis? How do some members of a colony of starving amoeba send out a target and spiral wave signal to attract neighboring amoebae and transform them into spores, and then to regenerate into amoeba again when food (bacteria) becomes available? How does a “scroll wave” get generated in the cardiac muscle by the inadvertent presence of an electrical impulse during a *vulnerable window* of a few milliseconds, often leading to sudden cardiac death?

The above phenomena are some manifestations of a multidisciplinary paradigm called *emergence*, or *complexity*. They share a common unifying principle characteristic of *dynamic arrays*, such as *cellular neural networks*, namely, interconnections of a sufficiently large numbers of *simple* dynamical units, which can exhibit extremely complex, synergetic, and *self-organizing* behaviors. The common denominator in all of these pattern formation and active wave propagation phenomena is the presence of an *active medium*, powered by a constant supply of external energy. For example, in the brain, the active medium is provided by a sheet-like array of massively interconnected excitable neurons whose energy comes from the burning of glucose with oxygen. In cellular neural networks, the active medium is provided by the local interconnections of active cells, whose building blocks include *active* nonlinear devices (e.g., CMOS transistors) powered by batteries.

Research on *Emergence* and *Complexity* has gained immense momentum during the past decade<sup>1-15</sup>. The fundamental problem is to uncover nature's secret mechanisms which are responsible for the self organization and spontaneous emergence of many stable complex (*static* and *dynamic*) patterns<sup>a</sup> in homogeneous media operating *far-from-thermodynamic equilibrium*<sup>16</sup>. Indeed, nature is abound with all sorts of patterns ranging from regular snow flakes to chaotic brain waves<sup>17,18,19</sup>. Understanding and controlling such patterns is essential for designing new generations of brain-like molecular devices and systems endowed with artificial intelligence and self-repair capabilities.

The *homogeneous* media alluded to above consists usually of an active *bulk* medium (e.g., bulk materials with *negative* resistivity, such as Gallium Arsenide in Gunn Diodes<sup>20</sup>, nerve membranes, heart tissue layers, chemical mixtures in stirred reactor tanks, etc.) modeled by one or more nonlinear *PDE*'s (partial differential equations) where the spatial coordinate, as well as the state variables, are represented by *continuous real numbers*. What is truly fascinating is that while these active media are completely unrelated—they can range from inanimate materials to living tissues<sup>21</sup>—yet the patterns they exhibit tend to resemble each other under appropriate initial and boundary conditions. It makes sense therefore to hypothesize that a common mechanism must be responsible for the emergence of each type of patterns (e.g., Turing patterns, spiral waves, etc.)<sup>b</sup>. This remarkable observation motivates the development of a *unified paradigm* capable of exhibiting most, if not all, static and dynamic patterns (i.e., *dissipative structures*) in active homogeneous media operating far from thermodynamic equilibrium. Such a paradigm has been developed recently and is the subject of a recent treatise<sup>22</sup>. The paradigm is dubbed the *CNN*, an acronym for *cellular neural networks* when used in the context of brain science, or *cellular nonlinear networks*, when used in other more general contexts.

A CNN is defined by *two* mathematical constructs:

1. A spatially discrete collection of nonlinear dynamical systems called *cells*, where *information* can be encrypted into each cell via 3 independent variables

<sup>a</sup>Such patterns are called *dissipative structures* by Ilya Prigogine<sup>14</sup> because *energy must be continually supplied and dissipated* in order to maintain such structures.

<sup>b</sup>For related works on emergence and complexity from different perspectives, the reader is referred to the very readable expositions by Crick<sup>8</sup>, Eigen<sup>10</sup>, Gell-Mann<sup>7</sup>, and Prigogine<sup>14</sup>.

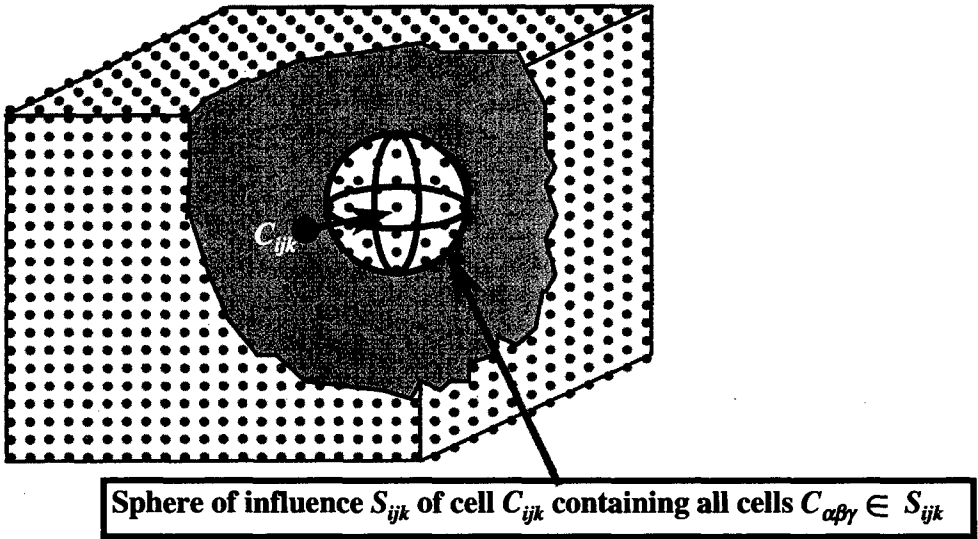


Figure 1. A CNN with a cutout view which exposes an inner cell  $C_{ijk}$  and its sphere of influence  $S_{ijk}$ . Only those cells  $C_{\alpha\beta\gamma}$  located within  $S_{ijk}$  are coupled to cell  $C_{ijk}$ .

called *input*, *threshold*, and *initial state*.

2. An *interconnection law* relating one or more relevant variables of each cell  $C_{ij}$  to all neighbor cells  $C_{kl}$  located within a prescribed sphere of influence  $S_{ij}(r)$  of radius  $r$ , centered at  $C_{ij}$ .

In the special case where the CNN consists of a homogeneous array, and where its cells have no inputs, no thresholds, and no outputs, and where the sphere of influence extends only to the *nearest* neighbors (i.e.,  $r = 1$ ), the CNN reduces to the familiar concept of a *lattice dynamical system* from mathematics.

The schematic diagram of a 3-dimensional CNN is shown in Fig.1, where a typical cell  $C_{ijk}$  is highlighted along with its *sphere of influence*  $S_{ijk}$ . Let us consider some examples.

#### *Example 1. Emergence of 3-Dimensional Knot Patterns*

Suppose each cell in Fig.1 consists of a Chua's circuit with three external terminals (one of them being the *ground* reference terminal), as shown in Fig.2. Since each cell can interact with its neighbors only through the 2 ungrounded terminals, each one coupled to a corresponding node of a neighbor cell via a resistor, each ungrounded terminal serves as a *port* where energy can flow into or out of the cell. Consequently, the 3-terminal circuit cell in Fig.3 is also called a 2-port in electrical engineering. Suppose each cell in Fig.2 is *coupled* to its 6 nearest neighbor cells (two along each coordinate axis) via positive linear resistances, as depicted in Fig.2.

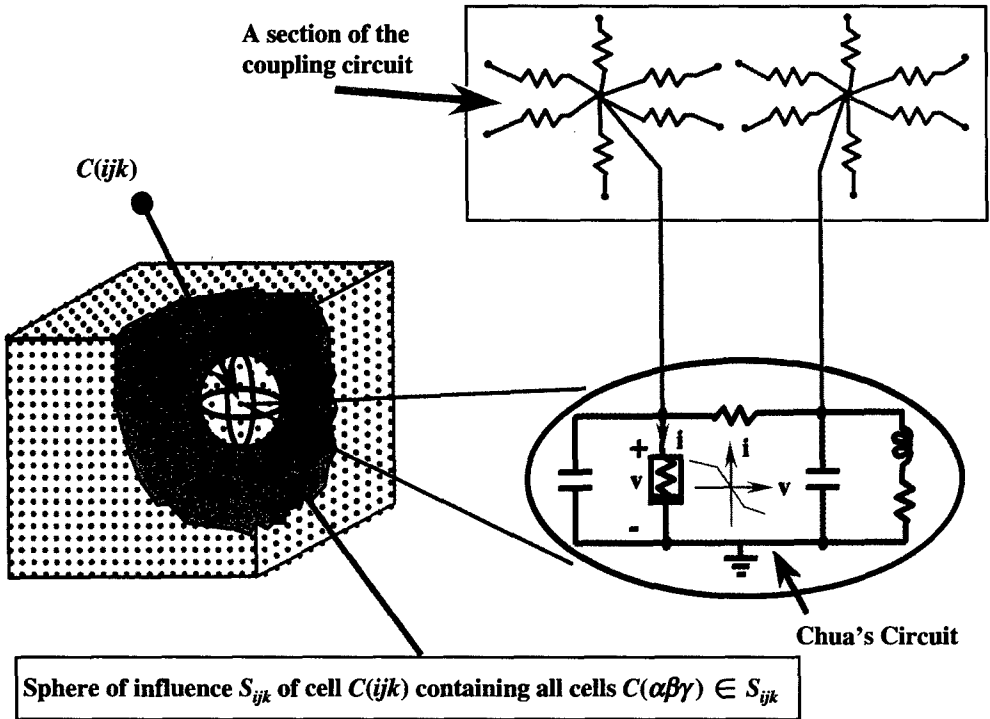
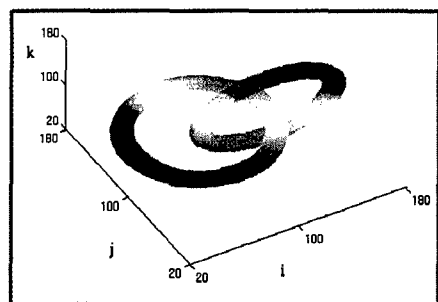


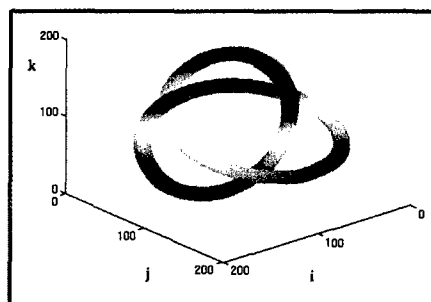
Figure 2. Each cell in this 3-dimensional CNN is a Chua's oscillator with 3 external terminals, or 2 ports, with a common ground. Each external terminal (except the ground), or port, of each cell is connected to a capacitor inside the cell, and *coupled* to a corresponding terminal of the 6 neighboring cells via 6 linear passive resistors.

If all elements inside the cell shown in the inset are passive, and if the nonlinear resistor is *not locally active* (e.g., a pn junction diode) in the sense of *Definition 1* in Sec.4.2, then it can be shown that given any *initial* voltage distributions, all node-to-datum voltages must tend to zero as  $t \rightarrow \infty$ . In other words, this CNN must have a *homogeneous* (uniform) solution at all nodes. This homogeneity is generally expected since all cells in Fig.7, and their couplings, as well as boundary conditions, are identical, and there are *no input sources*.<sup>c</sup>

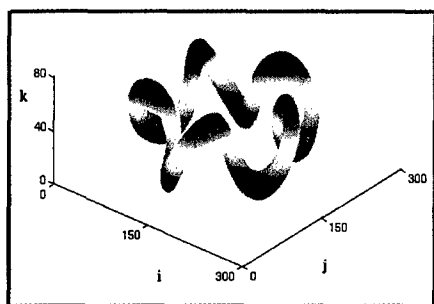
<sup>c</sup>We assume throughout this paper that the CNN has no input sources and has a symmetrical boundary condition (e.g., a zero-flux or Neumann boundary condition), since the central concept of *emergence* implies that any non-homogeneous output pattern must emerge via *self organization*, and not through any external input, or non-symmetrical boundary conditions.



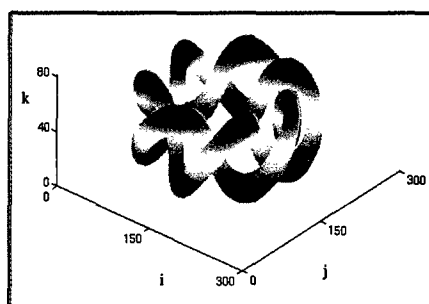
(a)



(b)



(c)



(d)

Figure 3. Three-dimensional *knot* voltage distribution patterns from a CNN cube made of Chua's oscillator cells, coupled via a linear passive resistive grid. (a) A Hopf-link pattern. (b) A 3-knot pattern. (c) A simple helix. (d) A double helix.

However, if the nonlinear resistor is chosen to be a Chua's diode<sup>23</sup>, as shown in the inset in Fig.2, then for the *fixed* choice of circuit parameters<sup>22</sup>, the 4 distinctly different 3-dimensional structures in Fig.3 can be obtained in steady state by choosing the 4 different sets of initial conditions<sup>22</sup>. Note that this CNN is symmetrical with respect to the center of the CNN cube in Fig.2 and there are no inputs. Yet we have a non-uniform constant steady state node-to-datum voltage distribution ! In the parlance of *complexity theory*, we say the homogeneous CNN undergoes a *symmetry breaking* and any *non-homogeneous* node-to-datum steady state voltage distribution is called a *pattern*, or a *dissipative structure* if the medium is *non-conservative* in the sense that *energy dissipation* is essential to maintain the structure.

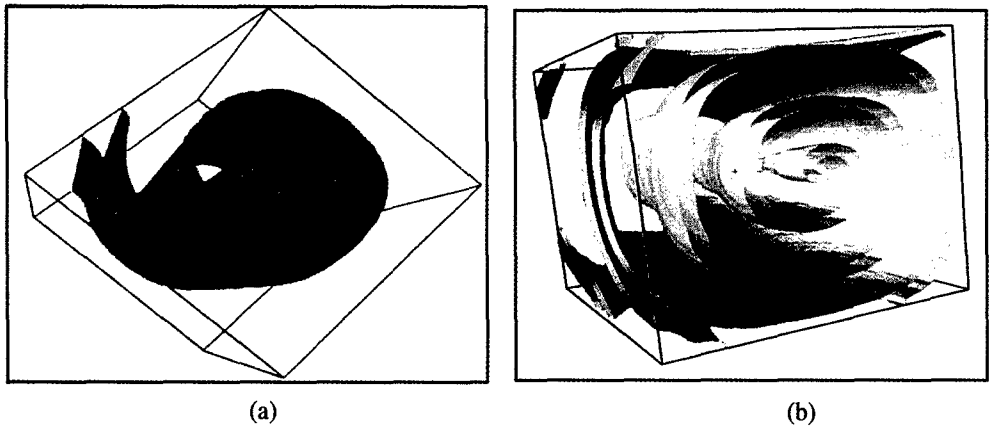


Figure 4. (a) A straight scroll vortex. (b) A twisted scroll wave.

#### *Example 2. Emergence of 3-Dimensional Scroll Waves*

Consider the same CNN cube as in Fig.2 except that in this case, only the port voltage across the nonlinear resistor (Chua's diode) is coupled to corresponding node voltages of the 6 neighboring cells. This is equivalent to *open circuiting* the second port (on the right) of the Chua's oscillator in Fig.2, so that each cell reduces to a *one-port* circuit with 2 external terminals (including the ground reference terminal). Using the *circuit parameters*, and the *initial* and *boundary* conditions<sup>22</sup>, we obtain the two *scroll wave* structures shown in Figs.4(a) and 4(b), respectively, for one instant of time. Unlike the *stationary* structures shown in Fig.3, the scroll waves in Fig.4 represent an *active nonlinear wave* which evolves continuously with a scrolling structure at all times.

#### *Example 3. Emergence of 2-Dimensional Spiral Waves*

If we consider a 2-dimensional version of the preceding CNN cube, we would obtain the simplified 2-dimensional CNN shown in Fig.5, where each "Chua's oscillator"-one-port is represented by a 2-terminal black box, coupled to its neighbors by 4 linear positive resistances, two along each coordinate axis. Using the circuit parameters and the initial and boundary conditions given in<sup>22</sup>, we obtain the *spiral wave* structure shown in Fig.6. Again, this is a *dynamic pattern* which rotates continuously for all times.

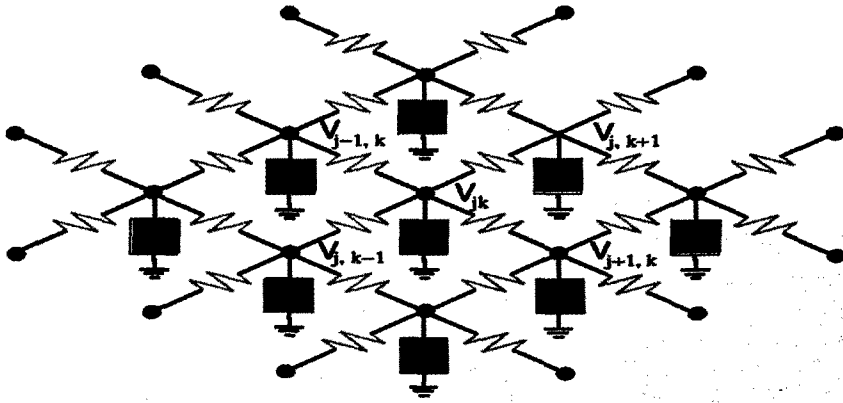


Figure 5. A two-dimensional CNN made of Chua's oscillator cells coupled via a single layer of linear resistive grid.

## 2 Mapping PDE Into CNN

A vast majority of active homogeneous media which are known to exhibit complexity in the form of *dissipative structures* are modeled by a *reaction diffusion PDE*<sup>14-18</sup>:

$$\frac{\partial x_i}{\partial t} = f_i(x_1, x_2, \dots, x_n) + D_i \left( \frac{\partial^2 x_i}{\partial x^2} + \frac{\partial^2 x_i}{\partial y^2} + \frac{\partial^2 x_i}{\partial z^2} \right),$$

$$i = 1, 2, \dots, n \quad (1)$$

where  $\mathbf{x} = (x_1, x_2, \dots, x_n)^T$  are state variables,  $(x, y, z)$  are spatial coordinates,  $\mathbf{f}(\mathbf{x}) = (f_1(\mathbf{x}), f_2(\mathbf{x}), \dots, f_n(\mathbf{x}))$  is a nonlinear vector function of  $\mathbf{x}$  called the *kinetic term*, and  $D_1, D_2, \dots, D_n$  are constants called *diffusion coefficients*. Replacing the *Laplacian* in Eq.(1) by its *discretized* version

$$\frac{\partial^2 x_i}{\partial x^2} + \frac{\partial^2 x_i}{\partial y^2} + \frac{\partial^2 x_i}{\partial z^2} \rightarrow (\nabla^2 \mathbf{x}_{\alpha, \beta, \gamma})_i \quad (2)$$

where

$$\begin{aligned} \nabla^2(\mathbf{x}_{\alpha,\beta,\gamma})_i &\triangleq x_i(\alpha+1, \beta, \gamma) + x_i(\alpha-1, \beta, \gamma) + x_i(\alpha, \beta+1, \gamma) + x_i(\alpha, \beta-1, \gamma) + \\ &\quad x_i(\alpha, \beta, \gamma+1) + x_i(\alpha, \beta, \gamma-1) - 6x_i(\alpha, \beta, \gamma) \\ i &= 1, 2, \dots, n \end{aligned} \quad (3)$$

is the discrete *Laplacian operator* on the  $i$ th component  $x_i$  of the state variable  $\mathbf{x} = (x_1, x_2, \dots, x_n)^T$  about the grid point with spatial coordinate  $(\alpha, \beta, \gamma)$ . We obtain the following associated *Reaction Diffusion CNN* equation

$$\begin{aligned} \dot{x}_i(\alpha, \beta, \gamma) &= f_i(x_1(\alpha, \beta, \gamma), x_2(\alpha, \beta, \gamma), \dots, x_n(\alpha, \beta, \gamma)) + D_i \nabla^2(\mathbf{x}_{\alpha,\beta,\gamma})_i \quad (4) \\ \text{where } i &= 1, 2, \dots, n; \alpha = (1, 2, \dots, N_\alpha), \beta = (1, 2, \dots, N_\beta), \text{ and } \gamma = (1, 2, \dots, N_\gamma). \end{aligned}$$

Here  $x_i(\alpha, \beta, \gamma)$  denotes the state variable  $x_i$  located at a point in the 3-dimensional space with spatial coordinate  $(\alpha, \beta, \gamma)$ . Observe that the Reaction Diffusion CNN equation (4) consists of a system of  $N = nN_\alpha N_\beta N_\gamma$  ordinary differential equations (ODE's).

We will henceforth refer to the process of transforming a PDE into a CNN equation as *mapping a PDE into a CNN*. Table 1 shows the mapping of 4 well-known reaction diffusion PDE's.

Table 1. Mapping Reaction-Diffusion PDE into a Reaction Diffusion CNN.

<i>FitzHugh-Nagumo CNN Equation</i>	<i>FitzHugh-Nagumo PDE</i>
$\begin{aligned} \dot{u}_i &= -\left(\frac{u_i^3}{3} - u_i\right) - v_i \\ &\quad + D_1[u_{i+1} + u_{i-1} - 2u_i] \\ \dot{v}_i &= -\epsilon[u_i - bv_i + a] \end{aligned}$	$\begin{aligned} \frac{\partial u}{\partial t} &= -\left(\frac{u^3}{3} - u\right) - v + D_1 \frac{\partial^2 u}{\partial x^2} \\ \frac{\partial v}{\partial t} &= -\epsilon[u - bv + a] \end{aligned}$
<i>Brusselator CNN Equation</i>	<i>Brusselator PDE</i>
$\begin{aligned} \dot{u}_{ij} &= a - (b+1)u_{ij} + u_{ij}^2 v_{ij} + D_1[u_{i+1,j} \\ &\quad + u_{i-1,j} + u_{i,j+1} + u_{i,j-1} - 4u_{ij}] \\ \dot{v}_{ij} &= bu_{ij} - u_{ij}^2 v_{ij} + D_2[v_{i+1,j} \\ &\quad + v_{i-1,j} + v_{i,j+1} + v_{i,j-1} - 4v_{ij}] \end{aligned}$	$\begin{aligned} \frac{\partial u}{\partial t} &= a - (b+1)u + u^2 v + D_1 \left[ \frac{\partial^2 u}{\partial x^2} + \frac{\partial^2 u}{\partial y^2} \right] \\ \frac{\partial v}{\partial t} &= bu - u^2 v + D_2 \left[ \frac{\partial^2 v}{\partial x^2} + \frac{\partial^2 v}{\partial y^2} \right] \end{aligned}$
<i>Meinhardt-Gierer CNN Equation</i>	<i>Meinhardt-Gierer PDE</i>
$\begin{aligned} \dot{u}_{ij} &= \frac{\alpha u_{ij}^2}{v_{ij}} - \beta u_{ij} + D_1[u_{i+1,j} + u_{i-1,j} \\ &\quad + u_{i,j+1} + u_{i,j-1} - 4u_{ij}] \\ \dot{v}_{ij} &= \alpha u_{ij}^2 - \gamma v_{ij} + D_2[v_{i+1,j} + v_{i-1,j} \\ &\quad + v_{i,j+1} + v_{i,j-1} - 4v_{ij}] \end{aligned}$	$\begin{aligned} \frac{\partial u}{\partial t} &= \frac{\alpha u^2}{v} - \beta u + D_1 \left[ \frac{\partial^2 u}{\partial x^2} + \frac{\partial^2 u}{\partial y^2} \right] \\ \frac{\partial v}{\partial t} &= \alpha u^2 - \gamma v + D_2 \left[ \frac{\partial^2 v}{\partial x^2} + \frac{\partial^2 v}{\partial y^2} \right] \end{aligned}$

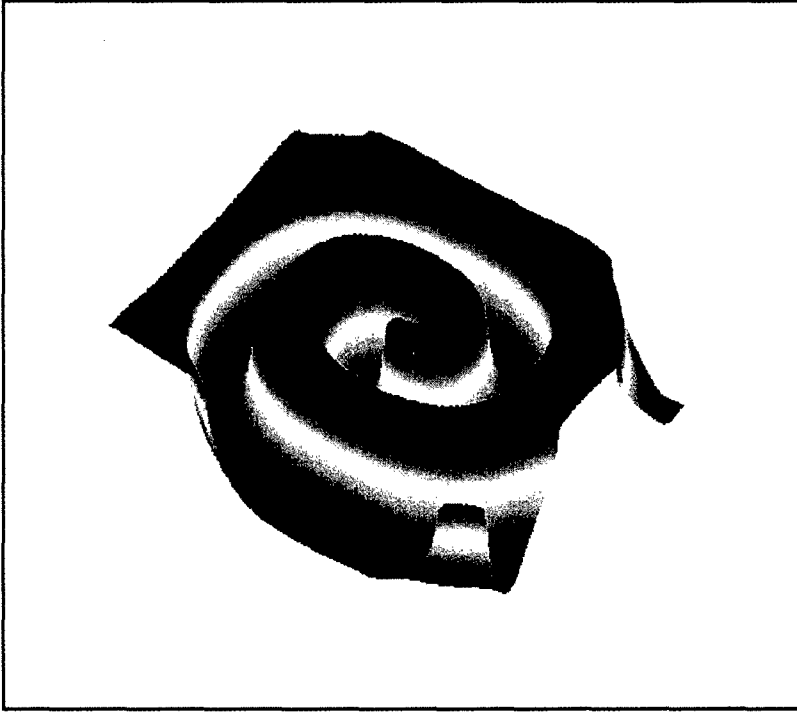


Figure 6. Three-dimensional view of a steadily rotating spiral wave at one instant of time. The vertical axis (perpendicular to the plane) represents the capacitor voltage across Chua's diode and the horizontal axes (on the plane) are the spatial coordinates.

<i>Oregonator CNN Equation</i>	<i>Oregonator PDE</i>
$\begin{aligned} \epsilon \dot{u}_{ijk} = & u_{ijk} + v_{ijk} - \alpha u_{ijk}^2 - u_{ijk}v_{ijk} + \\ & D_1[u_{i+1,j,k} + u_{i-1,j,k} + u_{i,j+1,k} \\ & + u_{i,j-1,k} + u_{i,j,k+1} + u_{i,j,k-1} \\ & - 6u_{ijk}] \end{aligned}$	$\begin{aligned} \epsilon \frac{\partial u}{\partial t} = & u + v - \alpha u^2 - uv \\ & + D_1 \left[ \frac{\partial^2 u}{\partial x^2} + \frac{\partial^2 u}{\partial y^2} + \frac{\partial^2 u}{\partial z^2} \right] \end{aligned}$
$\begin{aligned} \dot{v}_{ijk} = & -v_{ijk} + \beta w_{ijk} - u_{ijk}v_{ijk} + \\ & D_2[v_{i+1,j,k} + v_{i-1,j,k} + v_{i,j+1,k} \\ & + v_{i,j-1,k} + v_{i,j,k+1} + v_{i,j,k-1} \\ & - 6v_{ijk}] \end{aligned}$	$\begin{aligned} \frac{\partial v}{\partial t} = & -v + \beta w - uv \\ & + D_2 \left[ \frac{\partial^2 v}{\partial x^2} + \frac{\partial^2 v}{\partial y^2} + \frac{\partial^2 v}{\partial z^2} \right] \end{aligned}$
$\begin{aligned} \dot{w}_{ijk} = & u_{ijk} - w_{ijk} + D_3[w_{i+1,j,k} \\ & + w_{i-1,j,k} + w_{i,j+1,k} + w_{i,j-1,k} \\ & + w_{i,j,k+1} + w_{i,j,k-1} - 6w_{ijk}] \end{aligned}$	$\begin{aligned} \frac{\partial w}{\partial t} = & u - w \\ & + D_3 \left[ \frac{\partial^2 w}{\partial x^2} + \frac{\partial^2 w}{\partial y^2} + \frac{\partial^2 w}{\partial z^2} \right] \end{aligned}$

Reaction diffusion PDE's form an important, albeit relatively small, subset of the universe of all nonlinear PDE's. For any other nonlinear PDE, the *spatial derivative* (of any order) of any *state variable*  $u_i(t; x, y, z)$  at *time*  $t$  and *spatial location*  $^d (x, y, z) \in \mathbf{R}^3$  can be *approximated* to any desired accuracy <sup>24,25</sup> by *finite differences* involving only the values of the state variable  $u_i(t; \alpha', \beta', \gamma')$  located at a *finite number* of lattice points  $(x, y, z) = (\alpha', \beta', \gamma') \in S_{\alpha\beta\gamma}$ , where  $(\alpha, \beta, \gamma) \in \mathbf{Z}^3$  denotes the "discrete" coordinates of a 3-dimensional lattice  $\mathbf{Z}^3$ , and  $S_{\alpha\beta\gamma}(r)$  denotes a neighborhood of radius  $r$ , centered at  $(\alpha, \beta, \gamma)$ . Hence, given any nonlinear PDE, we can generate many (depending on the desired accuracy) approximate discretized systems of ODE's in terms of a 3-dimensional array of state variables  $x_i(\alpha, \beta, \gamma)$ ,  $\alpha = 1, 2, \dots, N_\alpha$ ,  $\beta = 1, 2, \dots, N_\beta$ ,  $\gamma = 1, 2, \dots, N_\gamma$ . Moreover, since all *finite-difference* operations involve only variables located within a *local* neighborhood, we can always *decompose*<sup>e</sup> the discretized system into a component (the *isolated cell*) which involves only  $u_i(t; \alpha, \beta, \gamma)$  at the lattice site  $(\alpha, \beta, \gamma)$ , and another component (the *cell coupling*) which involves all neighboring cells  $(\alpha', \beta', \gamma') \in S_{\alpha\beta\gamma}(r)$ . In other words, given any nonlinear PDE, we can induce many *associated CNN equations*— the examples given in *Table 1* represent the simplest examples. Although it is *not true* that the qualitative behaviors of a nonlinear PDE and its associated CNN equation are always the same—the propagation failure phenomenon<sup>26</sup> is a case in point, extensive computer experiments have shown that for the vast majority of cases, the respective solutions can be made virtually indistinguishable by choosing a sufficiently large array size and by optimizing the CNN cell and coupling parameters <sup>22</sup>.

It is important to observe that partial differential equations are merely mathematical abstractions of nature. The concept of a *continuum* is in fact an idealization of reality. Even the collection of all electrons in a solid does not form a continuum because much of the volume separating the electrons from the nucleus of atoms<sup>f</sup> represents a vast empty space! In fact, recent works by Smolin and his colleagues have proved that "*the spectrum of the volume of any physical region is discrete*"<sup>27</sup>. In particular, quantum mechanics implies that at extremely small distances even space is made of discrete bits!

### 3 Local Activity Is the Origin of Complexity

Let  $\mathcal{N}$  be a 2-dimensional CNN associated with a homogeneous medium. By definition, a CNN is defined uniquely by *cells* and their *interactions*. Let us identify each cell  $C(j, k)$  as a nonlinear *m-port* defined by its cell dynamics, where  $m$  is equal to the number of state variables which are *directly coupled* to its neighbors, as depicted by the " $m$ " external (ungrounded) terminals attached to each cell  $C(j, k)$  in Fig.7 for a reaction diffusion CNN. Note that the cell  $C(j, k)$  may contain additional state

<sup>d</sup>To avoid clutter we restrict our discussion to the 3-dimensional Euclidean space  $\mathbf{R}^3$ . The same formulation is valid for any dimension.

<sup>e</sup>In most cases, the decomposition consists of just the superposition of these two components. However, more complex decompositions (e.g., nonlinear functional compositions) may be required for some nonlinear PDE's.

<sup>f</sup>The ratio between the diameter of the electron orbits in an atom to the diameter of its nucleus is of the order of  $10^5$ .

variables which are not directly coupled to its neighbors and hence are suppressed in Fig.7 to avoid clutter.<sup>9</sup>

Let us identify next the *couplings* from cell  $C(j, k)$  to all cells within the  $3 \times 3$  sphere of influence  $S_{jk}$  centered at  $(j, k)$  by a  $\gamma$ -port  $\Gamma_{jk}$ . For the one-diffusion reaction diffusion CNN shown in Fig.5, an isolated cell  $C(j, k)$  and its 4 coupling resistors are shown in Fig.8(a). Note that the 5-terminal coupling circuit, or  $\gamma$ -port  $\Gamma_{jk}$  ( $\gamma = 4$  in this case), in Fig.8(a) can be redrawn into the form of a *grounded* 4-port (i.e., with a common ground terminal) in Fig.8(b). For the reaction-diffusion CNN depicted in Fig.7, the  $\gamma$ -port  $\Gamma_{jk}$  is composed of  $m$  identical grounded 4-ports (with node  $(j, k)$  as the ground node) made of 4 identical positive resistances, so that  $\gamma = 4m$ . Observe that a CNN is completely specified by the  $m$ -port cell  $C(j, k)$  and the  $\gamma$ -port coupling  $\Gamma_{jk}$  since they can be used as a template to build up a CNN of any array size.

Since the conductance of all resistors in each layer " $i$ " of the resistive grid in Fig.7 is equal to the diffusion coefficient  $D_i$ , which is assumed to be positive, it follows that the  $\gamma$ -port coupling  $\Gamma_{jk}$  is passive. If the cell  $C(j, k)$  is *not locally active*, then it follows from symmetry considerations and the qualitative theory of nonlinear networks<sup>28,29,30,31</sup> that the CNN must have a *unique* steady state solution, thereby implying that all nodes belonging to the same layer must have identical node-to-datum voltages. It follows that no patterns or dissipative structures can exist.

In the general case, the  $\gamma$ -port coupling  $\Gamma_{jk}$  may consist of a *nonlinear dynamical* multi-port. In this case, the dynamics must again tend to a *homogeneous* node voltage distribution on each resistor grid if both the  $m$ -port cell  $C(j, k)$  and the  $\Gamma$ -port coupling  $\Gamma_{jk}$  are *not locally active*. The above analysis justifies the following fundamental result on complexity:

#### *The Local Activity Principle*

A CNN associated with a homogeneous non-conservative (i.e., *not lossless*) medium having a *zero-flux* boundary condition can *not* exhibit patterns or dissipative structures unless the *cells*, or the *couplings*, are *locally active*.

## 4 Local Activity for Reaction-Diffusion CNNs

In general, each cell  $C(j, k, l)$  in a reaction-diffusion CNN has  $n$  state variables but only  $m \leq n$  among them are coupled directly to its nearest neighbors via diffusion.

<sup>9</sup>A state variable  $x_k$  is suppressed if its associated diffusion coefficient  $D_k$  is zero.

In this case, the state equation of each cell  $C(j, k, l)$  assumes the form

$$\left. \begin{aligned}
 \dot{V}_1(j, k, l) &= f_1(V_1(j, k, l), V_2(j, k, l), \dots, V_n(j, k, l)) + D_1 \nabla^2 V_1(j, k, l) \\
 \dot{V}_2(j, k, l) &= f_2(V_1(j, k, l), V_2(j, k, l), \dots, V_n(j, k, l)) + D_2 \nabla^2 V_2(j, k, l) \\
 &\vdots \\
 \dot{V}_m(j, k, l) &= f_m(V_1(j, k, l), V_2(j, k, l), \dots, V_n(j, k, l)) + D_m \nabla^2 V_m(j, k, l) \\
 \dot{V}_{m+1}(j, k, l) &= f_{m+1}(V_1(j, k, l), V_2(j, k, l), \dots, V_n(j, k, l)) \\
 &\vdots \\
 \dot{V}_n(j, k, l) &= f_n(V_1(j, k, l), V_2(j, k, l), \dots, V_n(j, k, l)) \\
 j &= 1, 2, \dots, N_x; k = 1, 2, \dots, N_y; l = 1, 2, \dots, N_z.
 \end{aligned} \right\} \quad (5)$$

Alternatively, we can include the remaining Laplacian terms  $D_{m+1} \nabla^2 V_{m+1}(j, k, l)$ ,  $D_{m+2} \nabla^2 V_{m+2}(j, k, l)$ , ...,  $D_n \nabla^2 V_n(j, k, l)$  in Eq.(5) and set  $D_{m+1} = D_{m+2} = \dots = D_n = 0$ . Recasting Eq.(5) into vector form, we obtain

$$\dot{\mathbf{V}}_a = \mathbf{f}_a(\mathbf{V}_a, \mathbf{V}_b) + \mathbf{D}_a \nabla^2 \mathbf{V}_a \quad (6)$$

$$\dot{\mathbf{V}}_b = \mathbf{f}_b(\mathbf{V}_a, \mathbf{V}_b) \quad (7)$$

where

$$\mathbf{V}_a = [V_1(j, k, l), V_2(j, k, l), \dots, V_m(j, k, l)]^T \quad (8)$$

$$\mathbf{V}_b = [V_{m+1}(j, k, l), V_{m+2}(j, k, l), \dots, V_n(j, k, l)]^T \quad (9)$$

$$\mathbf{f}_a = [f_1(\cdot), f_2(\cdot), \dots, f_m(\cdot)] \quad (10)$$

$$\mathbf{f}_b = [f_{m+1}(\cdot), f_{m+2}(\cdot), \dots, f_n(\cdot)] \quad (11)$$

$$\nabla^2 \mathbf{V}_a = [\nabla^2 V_1(j, k, l), \nabla^2 V_2(j, k, l), \dots, \nabla^2 V_m(j, k, l)] \quad (12)$$

$$\mathbf{D}_a \triangleq \begin{bmatrix} D_1 & & & \\ & D_2 & & \\ & & \ddots & \\ & & & D_m \end{bmatrix}, D_i > 0 \quad (13)$$

To emphasize that a CNN is defined by specifying the dynamics of the *cells* and their *couplings* (*cell interaction laws*), let us rewrite Eqs.(6)-(7) into the following standard form <sup>32</sup>:

**cell dynamics:**

$$\dot{\mathbf{V}}_a = \mathbf{f}_a(\mathbf{V}_a, \mathbf{V}_b) + \mathbf{I}_a \quad (14)$$

$$\dot{\mathbf{V}}_b = \mathbf{f}_b(\mathbf{V}_a, \mathbf{V}_b) \quad (15)$$

cell interaction laws:

$$\begin{aligned} \mathbf{I}_a &= \mathbf{g}_a \left( \mathbf{V}_a(j, k, l), \mathbf{V}_a(j-1, k, l), \mathbf{V}_a(j+1, k, l), \mathbf{V}_a(j, k-1, l), \mathbf{V}_a(j, k+1, l), \right. \\ &\quad \left. \mathbf{V}_a(j, k, l-1), \mathbf{V}_a(j, k, l+1) \right) \\ &= \begin{bmatrix} D_1 & & & \\ & D_2 & & \\ & & \ddots & \\ & & & D_m \end{bmatrix} \begin{bmatrix} \nabla^2 V_1(j, k, l) \\ \nabla^2 V_2(j, k, l) \\ \vdots \\ \nabla^2 V_m(j, k, l) \end{bmatrix} \end{aligned} \quad (16)$$

It is important to observe that Eqs.(14)-(15) defining the *cell dynamics* involve only the voltage variables ( $\mathbf{V}_a(j, k, l), \mathbf{V}_b(j, k, l)$ ) and the current variables  $\mathbf{I}_a(j, k, l)$  at *the same* spatial location  $(j, k, l)$ ,<sup>h</sup> whereas Eq.(16) defining the *cell interaction laws* involves *not only* the voltage variable  $\mathbf{V}_a(j, k, l)$  at spatial location  $(j, k, l)$ , but also those of the neighboring cells. The relationship between a typical cell  $C(j, k, l)$  at location  $(j, k, l)$  and its *coupling* network is shown in Fig.7 for a 2-dimensional CNN reaction diffusion equation, where  $\mathbf{V}_a = [V_1(j, k), V_2(j, k), \dots, V_m(j, k)]^T$  and  $\mathbf{I}_a = [I_1(j, k), I_2(j, k), \dots, I_m(j, k)]^T$  are the “ $m$ ” port voltage and port current variables. In the special case when  $m = 1$ , Fig.7 reduces to Fig.8(a), where cell  $C(j, k)$  degenerates into a one-port.

#### 4.1 Cell Equilibrium Points

Let us define the *static characteristic* of an isolated CNN cell by setting  $\dot{\mathbf{V}}_a = 0$  and  $\dot{\mathbf{V}}_b = 0$  in Eqs.(14) and (15); namely,

$$\mathbf{f}_a(\mathbf{V}_a, \mathbf{V}_b) + \mathbf{I}_a = \mathbf{0} \quad (17)$$

$$\mathbf{f}_b(\mathbf{V}_a, \mathbf{V}_b) = \mathbf{0} \quad (18)$$

where  $\mathbf{V}_a \in \mathbf{R}^m$ ,  $\mathbf{I}_a \in \mathbf{R}^m$ ,  $\mathbf{V}_b \in \mathbf{R}^{n-m}$ ,  $\mathbf{f}_a \in \mathbf{R}^m$ ,  $\mathbf{f}_b \in \mathbf{R}^{n-m}$ . Solving Eq.(18) for  $\mathbf{V}_b$  in terms of  $\mathbf{V}_a$ , we obtain

$$\mathbf{V}_b = \mathbf{g}_a(\mathbf{V}_a) \quad (19)$$

where  $\mathbf{g}_a(\cdot)$  may be a *multi-valued* function of  $\mathbf{V}_a$ .

Substituting Eq.(19) for  $\mathbf{V}_b$  in Eq.17, we obtain the following *implicit* and possibly *multi-valued* function:

Static Cell  
Characteristic

$$\mathcal{G}(\mathbf{V}_a, \mathbf{I}_a) \triangleq \mathbf{f}_a(\mathbf{V}_a, \mathbf{g}_a(\mathbf{V}_a)) + \mathbf{I}_a = \mathbf{0} \quad (20)$$

<sup>h</sup>This observation allows us to suppress the spatial coordinates in Eqs.(14)-(15) without ambiguity.

Let us solve Eq.(20) for  $\mathbf{V}_a$ . In general, there can be many solutions  $\mathbf{V}_a = \mathbf{V}_a(Q_1), \mathbf{V}_a(Q_2), \dots, \mathbf{V}_a(Q_p)$  for each  $\mathbf{I}_a = \bar{\mathbf{I}}_a \in \mathbf{R}^m$ , where  $\mathbf{V}_a(Q_i)$  denotes the port voltage solution  $\mathbf{V}_a$  at the  $i$ th solution  $Q_i$ . We call each solution  $\mathbf{V}_a = \mathbf{V}_a(Q_i)$  a *cell equilibrium point* associated with  $\mathbf{I}_a = \bar{\mathbf{I}}_a \in \mathbf{R}^m$ . In other words, each cell equilibrium point  $\mathbf{V}_a(Q_i)$  is *parameterized* by  $\mathbf{I}_a \in \mathbf{R}^m$ . The loci of all such cell equilibrium points calculated *explicitly* at  $\mathbf{I}_a = \bar{\mathbf{I}}_a$ , as  $\bar{\mathbf{I}}_a$  ranges over the entire  $m$ -dimensional Euclidean space  $\mathbf{R}^m$  is identical to the static *cell characteristic* defined *implicitly* in Eq.(20).

#### 4.2 Cell Complexity Matrix

Let  $Q_i$  be a cell equilibrium point associated with  $\mathbf{I}_a = \mathbf{I}_a(Q_i)$ . Let  $\mathbf{V}_a(Q_i)$  (obtained from Eqs.(20)) be the corresponding cell equilibrium point of the cell state equations Eqs.(14)-(15). Let

$$\mathbf{J}(Q_i) \triangleq \begin{bmatrix} \mathbf{A}_{aa}(Q_i) & \mathbf{A}_{ab}(Q_i) \\ \mathbf{A}_{ba}(Q_i) & \mathbf{A}_{bb}(Q_i) \end{bmatrix} \quad (21)$$

denote the  $m \times m$  Jacobian matrix associated with  $\mathbf{f}_a(\mathbf{V}_a, \mathbf{V}_b)$  and  $\mathbf{f}_b(\mathbf{V}_a, \mathbf{V}_b)$ , evaluated at  $(\mathbf{V}_a(Q_i), \mathbf{V}_b(Q_i))$ , where  $\mathbf{V}_b(Q_i) = \mathbf{g}_a(\mathbf{V}_a)$  from Eq.(19), namely,

Small Signal CNN Cell  
Coefficients at  $Q_i$

$$\begin{aligned} \mathbf{A}_{aa}(Q_i) &= \left. \frac{\partial \mathbf{f}_a(\mathbf{V}_a, \mathbf{V}_b)}{\partial \mathbf{V}_a} \right|_{\mathbf{V}_a=\mathbf{V}_a(Q_i), \mathbf{V}_b=\mathbf{V}_b(Q_i)}, \\ \mathbf{A}_{ab}(Q_i) &= \left. \frac{\partial \mathbf{f}_a(\mathbf{V}_a, \mathbf{V}_b)}{\partial \mathbf{V}_b} \right|_{\mathbf{V}_a=\mathbf{V}_a(Q_i), \mathbf{V}_b=\mathbf{V}_b(Q_i)}, \\ \mathbf{A}_{ba}(Q_i) &= \left. \frac{\partial \mathbf{f}_b(\mathbf{V}_a, \mathbf{V}_b)}{\partial \mathbf{V}_a} \right|_{\mathbf{V}_a=\mathbf{V}_a(Q_i), \mathbf{V}_b=\mathbf{V}_b(Q_i)}, \\ \mathbf{A}_{bb}(Q_i) &= \left. \frac{\partial \mathbf{f}_b(\mathbf{V}_a, \mathbf{V}_b)}{\partial \mathbf{V}_b} \right|_{\mathbf{V}_a=\mathbf{V}_a(Q_i), \mathbf{V}_b=\mathbf{V}_b(Q_i)}. \end{aligned} \quad (22)$$

Let  $N(Q_i)$  be the linearized CNN cell at  $Q_i$  associated with the state Equations (14)-(15) of the  $m$ -port cell  $C(j, k, l)$  obtained by deleting the higher order terms in the Taylor series expansion of  $\mathbf{f}_a(\mathbf{V}_a, \mathbf{V}_b)$  and  $\mathbf{f}_b(\mathbf{V}_a, \mathbf{V}_b)$  about  $Q_i$ ; namely,

Linearized CNN Cell  
dynamics at  $Q_i$

$$\dot{\mathbf{v}}_a = \mathbf{A}_{aa}\mathbf{v}_a + \mathbf{A}_{ab}\mathbf{v}_b + \mathbf{i}_a \quad (23)$$

$$\dot{\mathbf{v}}_b = \mathbf{A}_{ba}\mathbf{v}_a + \mathbf{A}_{bb}\mathbf{v}_b \quad (24)$$

where  $\mathbf{v}_a \triangleq \mathbf{V}_a - \mathbf{V}_a(Q_i)$ ,  $\mathbf{v}_b \triangleq \mathbf{V}_b - \mathbf{V}_b(Q_i)$ ,  $\mathbf{i}_a \triangleq \mathbf{I}_a - \mathbf{I}_a(Q_i)$  are the infinitesimal voltages and currents, respectively, about the equilibrium point  $Q_i$ .

### Definition 1: Local Activity

A CNN cell  $C(j, k, l)$  is said to be *locally active* at  $Q_i$  iff there exists some  $\mathbf{i}_a(t)$  and some time  $T > 0$  such that

$$\delta\mathcal{E}(Q_i) \triangleq \int_0^T \langle \mathbf{v}_a(t), \mathbf{i}_a(t) \rangle dt < 0 \quad (25)$$

where  $\langle \cdot, \cdot \rangle$  denotes the vector dot product, and  $\mathbf{v}_a(t)$  is the solution obtained by solving Eqs.(23)-(24) under *zero initial state*  $\mathbf{v}_a(0) = \mathbf{0}$  and  $\mathbf{v}_b(0) = \mathbf{0}$ .

To derive a test for local activity, let us take the Laplace transform of Eq.(24) to obtain

$$s\hat{\mathbf{v}}_a(s) = \mathbf{A}_{aa}\hat{\mathbf{v}}_a(s) + \mathbf{A}_{ab}\hat{\mathbf{v}}_b(s) + \hat{\mathbf{i}}_a(s) \quad (26)$$

$$s\hat{\mathbf{v}}_b(s) = \mathbf{A}_{ba}\hat{\mathbf{v}}_a(s) + \mathbf{A}_{bb}\hat{\mathbf{v}}_b(s) \quad (27)$$

where  $\hat{\mathbf{v}}_a(s)$ ,  $\hat{\mathbf{v}}_b(s)$  and  $\hat{\mathbf{i}}_a(s)$  denote the Laplace transform of  $\mathbf{v}_a(t)$ ,  $\mathbf{v}_b(t)$ , and  $\mathbf{i}_a(t)$ , respectively. Solving for  $\hat{\mathbf{v}}_b(s)$  from Eq.(27), we obtain

$$\hat{\mathbf{v}}_b(s) = (s\mathbf{1} - \mathbf{A}_{bb})^{-1} \mathbf{A}_{ba}\hat{\mathbf{v}}_a(s) \quad (28)$$

Substituting Eq.(28) for  $\hat{\mathbf{v}}_b(s)$  in Eq.(26) and solving for  $\hat{\mathbf{i}}_a(s)$ , we obtain

$$\hat{\mathbf{i}}_a(s) = \mathbf{Y}_Q(s)\mathbf{v}_a(s) \quad (29)$$

where

CNN Cell Complexity Matrix at  $Q_i$

$$\mathbf{Y}_Q(s) \triangleq (s\mathbf{1} - \mathbf{A}_{aa}) - \mathbf{A}_{ab}(s\mathbf{1} - \mathbf{A}_{bb})^{-1} \mathbf{A}_{ba} \quad (30)$$

is called the *CNN cell complexity matrix* at the cell equilibrium point  $Q_i$ . It follows from a classic theorem in *circuit theory*<sup>33</sup> that for a *reaction diffusion CNN Cell* to be *locally active* at  $Q_i$ ,  $\mathbf{Y}_Q(s)$  should *not* be a *positive real matrix* at  $Q_i$ . Hence, in order for a reaction diffusion CNN equation to exhibit complexity, it is *necessary* that the cell parameters be chosen such that the *cell complexity matrix*  $\mathbf{Y}_Q(s)$  is *not* positive real at  $Q_i$ . The mathematical conditions for testing this local activity property is as follows:

*Local activity criteria for reaction diffusion CNN*

A Reaction Diffusion CNN Cell is *locally active* at a cell equilibrium point  $Q_i$  if, and only if, its cell complexity matrix  $\mathbf{Y}_Q(s)$ , or its inverse cell complexity matrix  $\mathbf{Z}_Q(s) \triangleq \mathbf{Y}_Q^{-1}(s)$  (In this case, simply change the symbol from  $\mathbf{Y}$  to  $\mathbf{Z}$  in the following 4 conditions) satisfies *any one* of the following 4 conditions:

1.  $\mathbf{Y}_Q(s)$  has a pole in  $Re[s] > 0$ .
2.  $\mathbf{Y}_Q^H(i\omega) \triangleq \mathbf{Y}_Q^\dagger(i\omega) + \mathbf{Y}_Q(i\omega)$  is *not* a positive semi-definite matrix at some  $\omega = \omega_0$ , where  $\omega_0$  is any real number, and  $\dagger$  denotes the Hermitian operator.
3.  $\mathbf{Y}_Q(s)$  has a *simple* pole  $s = i\omega_p$  on the *imaginary axis* where its associated *residue matrix*

$$\mathbf{K}_{-1} \triangleq \left. \begin{array}{l} \lim_{s \rightarrow i\omega_p} (s - i\omega_p) \mathbf{Y}_Q(s), \text{ if } \omega_p < \infty \\ \lim_{\omega_p \rightarrow \infty} \frac{\mathbf{Y}(i\omega_p)}{i\omega_p}, \text{ if } \omega_p = \infty \end{array} \right\}$$

is either *not* a Hermitian matrix, or else *not* a positive semi-definite Hermitian matrix.

4.  $\mathbf{Y}_Q(s)$  has a *multiple* pole on the imaginary axis.

*4.3 Reaction Diffusion CNN: One Diffusion Coefficient*

Many well-known reaction diffusion CNNs have only one non-zero diffusion coefficient and 2 state variables, i.e.,  $m = 1, n = 2$ . The most famous example belonging to this class is the FitzHugh Nagumo CNN Equation given in *Table 1*. For this class of reaction diffusion CNN, all variables in Eq.(24) are scalars and let us rewrite it using the established notation<sup>22</sup> for ease of reference:

$$\begin{aligned} \dot{v}_1 &= a_{11}v_1 + a_{12}v_2 + i_1 \\ \dot{v}_2 &= a_{21}v_1 + a_{22}v_2 \end{aligned} \quad (31)$$

The inverse *CNN cell complexity matrix*  $Y_Q^{-1}(s) \triangleq Z_Q(s) = \frac{\hat{v}_1(s)}{\hat{i}_1(s)}$  associated with Eq.(31) is a  $1 \times 1$  matrix, or scalar function of  $s$  in this case, and is given by

$$Z_Q(s) = \frac{(s - a_{22})}{s^2 - Ts + \Delta} \quad (32)$$

where

$$T = a_{11} + a_{22} \quad (33)$$

$$\Delta = a_{11}a_{22} - a_{12}a_{21} \quad (34)$$

are the *trace* and *determinant* of the associated Jacobian matrix

$$\mathbf{J}(Q_i) = \begin{bmatrix} a_{11} & a_{12} \\ a_{21} & a_{22} \end{bmatrix} \quad (35)$$

evaluated at the cell equilibrium point  $Q_i$ .

Applying the above *local activity criteria* to this special scalar case (with  $Y_Q(s)$  replaced by  $Z_Q(s)$ ), we obtain the following useful corollary:

*Local Activity Criteria for One Diffusion Coefficient* A one-port Reaction-Diffusion CNN cell with one diffusion coefficient and two state variables is *locally active* at a cell equilibrium point  $Q = (\bar{V}_1, \bar{I}_1)$  if, and only if, any one of the following 4 conditions holds at  $Q$ :

1.  $a_{11} + a_{22} > 0$  or  $a_{11}a_{22} < a_{12}a_{21}$ .
  2.  $a_{11} > 0$ , or  $a_{11} > \frac{a_{12}a_{21}}{a_{22}}$ , if  $a_{11} \leq 0$  and  $a_{22} \neq 0$ .
  3.  $a_{11}a_{22} > a_{12}a_{21}$ ,  $a_{11} + a_{22} = 0$  and  $a_{22} \neq 0$ .
  4.  $a_{11}a_{22} = a_{12}a_{21}$ ,  $a_{11} + a_{22} = 0$ , and  $a_{22} \neq 0$ .
- (36)

Although the above local activity criteria is couched in terms of the 4 Jacobian coefficients  $a_{11}$ ,  $a_{12}$ ,  $a_{21}$  and  $a_{22}$ , the criteria can be recast into the following 4 equivalent conditions involving only the 3 parameters  $\Delta$ ,  $T$ , and  $a_{22}$ :

- Equivalent condition 1:  $T > 0$ , or  
 $\Delta < 0$
- Equivalent condition 2:  $T > a_{22}$ , or  
 $T \leq a_{22}$  and  $a_{22}\Delta > 0$
- Equivalent condition 3:  $T = 0$ , and  
 $\Delta > 0$  and  
 $a_{22} \neq 0$  (37)
- Equivalent condition 4:  $T = 0$ , and  
 $\Delta = 0$  and  
 $a_{22} = 0$

To visualize the regions in the  $\Delta$ - $T$ - $a_{22}$  Euclidean space represented by the above system of inequalities, it is more convenient to consider a  $\Delta$ - $T$ - $a_{22}$  cylindrical sub-space and partition it into 8 uniform wedges above  $\Delta = 0$ , and 8 uniform wedges below  $\Delta = 0$ , as depicted in Fig.9. In terms of the  $\Delta$ - $T$ - $a_{22}$  cylinder, *Equivalent condition 1* is represented by all points  $(a_{22}, T, \Delta)$  behind the vertical separating plane  $T = 0$ , and all points below the horizontal separating plane  $\Delta = 0$ . *Equivalent condition 2* is represented by the wedges labeled 1, 2, 3, 4, 5, 7, and 8 in the upper half ( $\Delta > 0$ )

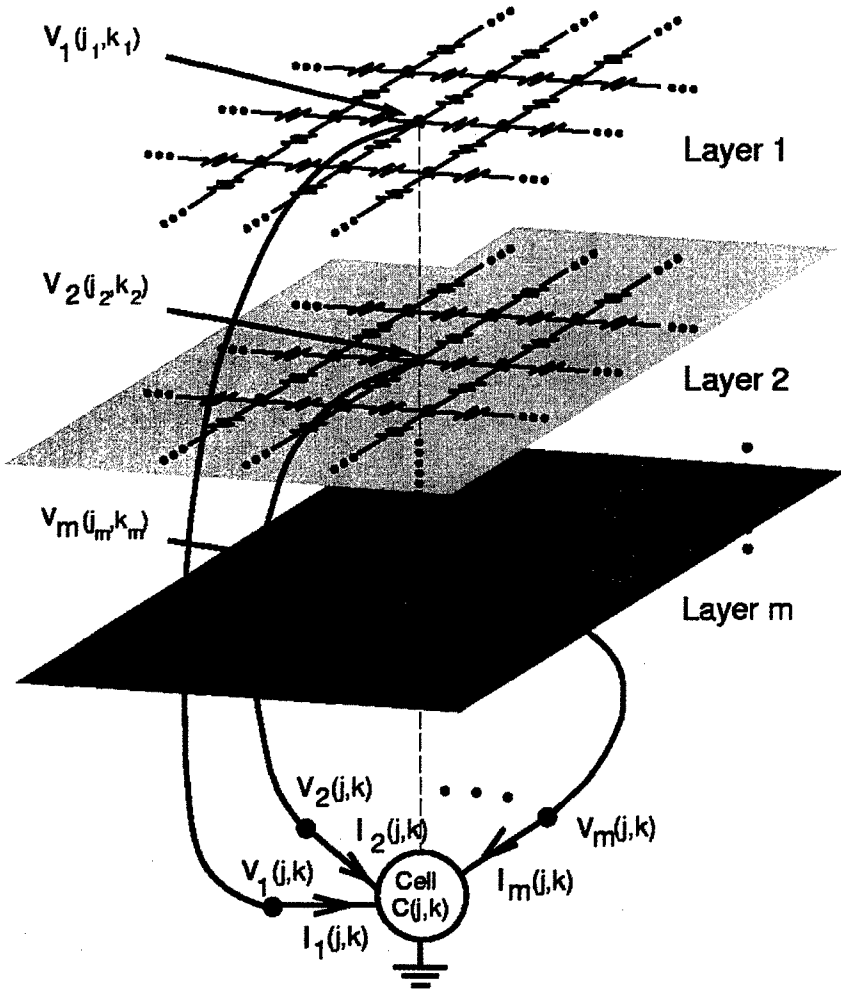


Figure 7. A 2-dimensional reaction-diffusion CNN having “ $m$ ” non-zero diffusion coefficients ( $D_i \neq 0, i = 1, 2, \dots, m$ ). The subscript “ $i$ ” attached to  $(j_i, k_i)$  denotes the node in the  $i$ th resistive grid layer which is connected to a terminal of cell  $C(j, k)$ . All resistors in layer  $i$  are linear resistors with identical conductance equal to  $D_i$  Siemens,  $i = 1, 2, \dots, m$ .

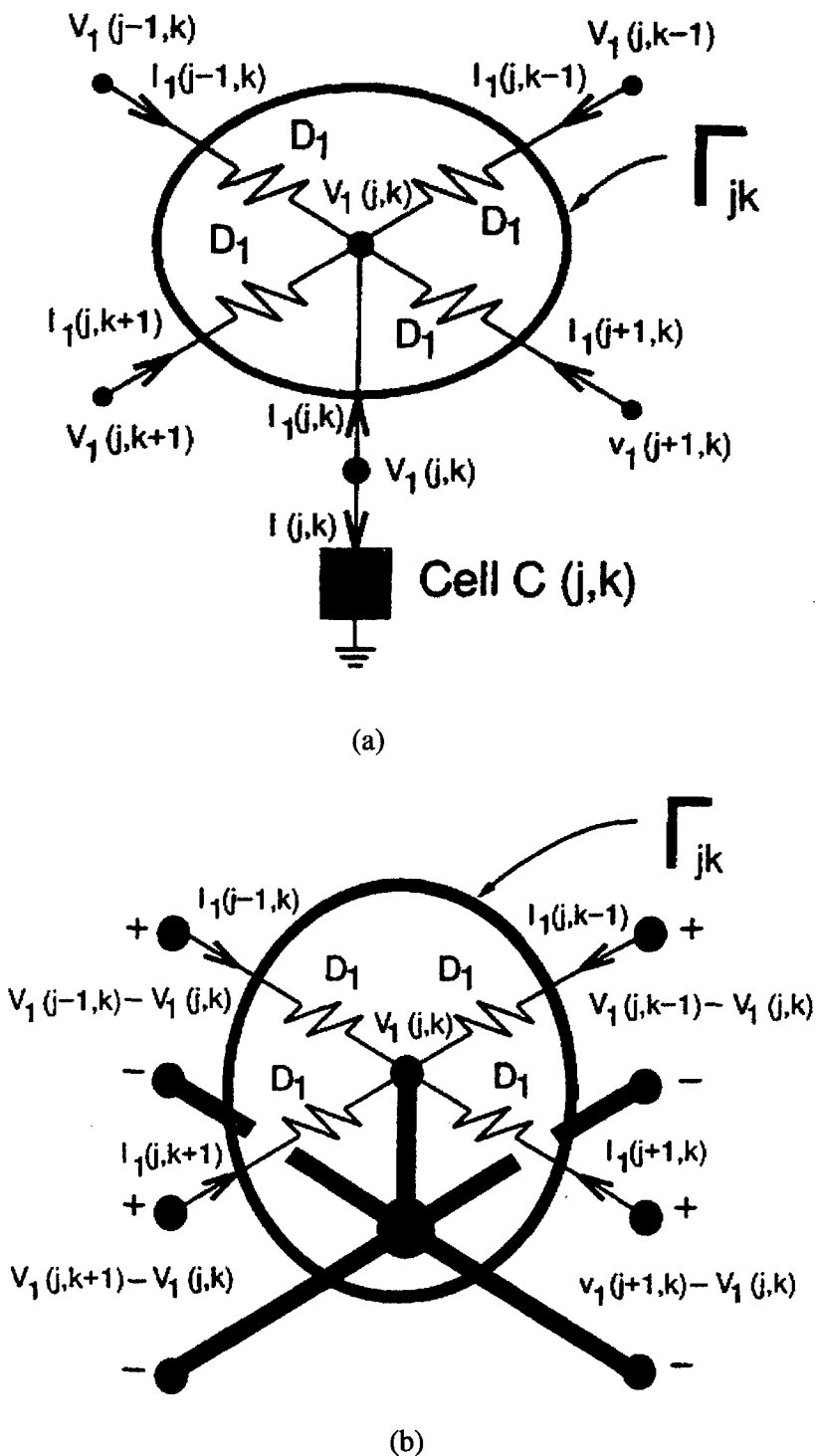


Figure 8. (a) An isolated cell  $C(j,k)$  from Fig.5 with its 4 coupling conductances  $D_1$ . (b) The 5-terminal circuit  $\Gamma_{jk}$  in (a) is equivalent to a 4-port where the bold wires form the common "ground" terminal of each port.

cylinder. *Equivalent condition 3* is represented by the vertical separating plane (excluding the vertical axis) in the upper half ( $\Delta > 0$ ) cylinder. *Equivalent condition 4* is represented by a single point at the origin. It follows from this partitioned cylinder that a reaction diffusion CNN with one diffusion coefficient and two state variables is *locally active* at a cell equilibrium point  $Q$  if, and only if, its associated parameter  $(a_{22}(Q), T(Q), \Delta(Q))$  at  $Q$  lies *outside* of the “blue” sector 6 in the upper half cylinder.

#### 4.4 Reaction Diffusion CNN: Two Diffusion Coefficients

Consider next the class of reaction diffusion CNNs with two diffusion coefficients ( $D_1 > 0$  and  $D_2 > 0$ ) and two state variables, i.e.,  $m = n = 2$ . Both the Brusselator and the Meinhardt-Gierer CNN equations in *Table 1* belong to this class. In this case, the CNN cell is a 3-terminal (including the ground reference terminal), or 2-port, device whose linearized cell dynamics about an equilibrium point  $Q_i$  is described by

$$\begin{aligned}\dot{v}_1 &= a_{11}v_1 + a_{12}v_2 + i_1 \\ \dot{v}_2 &= a_{21}v_1 + a_{22}v_2 + i_2\end{aligned}\quad (38)$$

where  $a_{11}$ ,  $a_{12}$ ,  $a_{21}$ , and  $a_{22}$  are the small-signal cell coefficients at  $Q_i$  defined in Eq.(35). Applying the *local activity criteria* from section 4.2 to the associated  $2 \times 2$  cell complexity matrix  $\mathbf{Y}_Q(s)$  at  $Q_i$ , we obtain the following corollary:

##### *Local activity criteria for two diffusion coefficients*

A two-port reaction-diffusion CNN cell with two diffusion coefficients and two state variables is *locally active* at a cell equilibrium point  $Q = (\bar{V}_1, \bar{V}_2, \bar{I}_1, \bar{I}_2)$  if, and only if, any one of the following two conditions holds at  $Q$ :

1.  $a_{22} > 0$
2.  $4a_{11}a_{22} < (a_{12} + a_{21})^2$

(39)

For a detailed application of the various local activity criteria presented in Sections 4.3 and 4.4 to concrete examples; namely, the FitzHugh-Nagumo Equation, the Brusselator Equation, and the Gierer-Mainhardt Equation, the reader is referred to <sup>34</sup>, <sup>35</sup>, and <sup>36</sup>, respectively.

## 5 Concluding Remarks

The preceding analysis can be generalized to any homogeneous media which can be mapped to a CNN defined by *any* cell dynamics, and *any* cell interaction laws, not necessarily of the reaction diffusion type presented in Section 4. In particular, the coupling  $\gamma$ -port  $\Gamma_{jkl}$  can be any *nonlinear dynamical* multi-port. In such cases, in order for the CNN to exhibit *complexity*, either the  $m$ -port cell  $C_{ijk}$ , or the

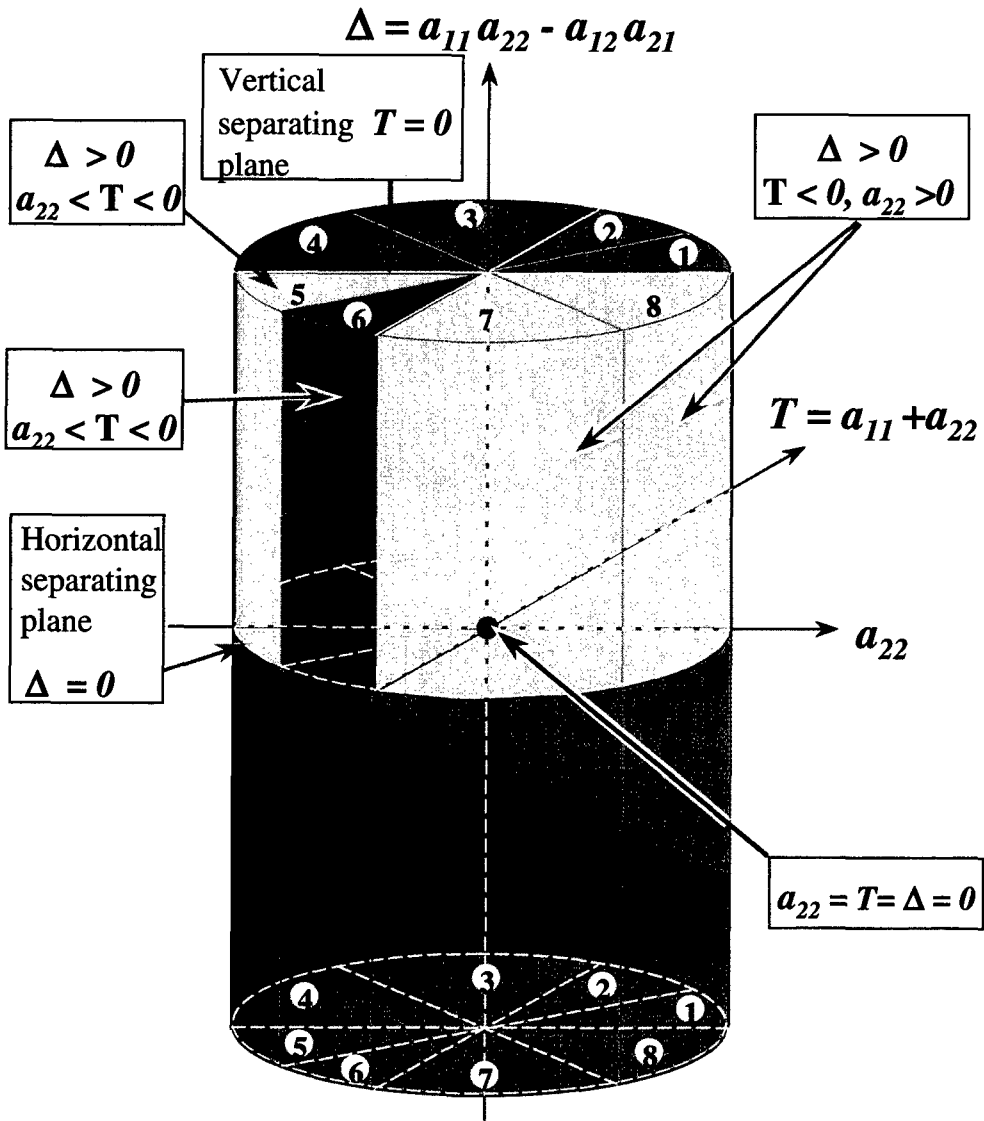


Figure 9. The  $\Delta$ - $T$ - $a_{22}$  cylinder depicting the *locally passive* region represented by wedge [6] in the upper half cylinder. All other regions are *locally active*. In particular, regions [5], [7], and [8] in the upper half cylinder  $\Delta > 0$  correspond to the *edge of chaos* where most complexities emerged.

coupling  $\gamma$ -port  $\Gamma_{ijk}$ , must be *locally active* at some *equilibrium point* of the *isolated* (disconnected from the rest of the CNN) *cell*  $C_{ijk}$ , or *isolated  $\gamma$ -port coupling*  $\Gamma_{jkl}$ .

While the CNN paradigm is an example of REDUCTIONISM *par excellence*, the true origin of emergence and complexity is traced to a much deeper new concept called *local activity*. The numerous complex phenomena unified under this mathematically precise principle include *self organization, dissipative structures, synergetics, order from disorder, far-from-thermodynamic equilibrium, collective behaviors, edge of chaos*, etc.

The central theme of the *local activity dogma* <sup>22</sup> asserts that the somewhat fuzzy notions of "emergence" and "complexity", as well as their various metamorphosis, such as those cited above, can all be rigorously explained by a precise scientific paradigm abstracted mathematically from the principle of conservation of energy; namely, a CNN operating near the *edge of chaos* <sup>34,37</sup>, where the cells are not only *locally active*, but also *linearly asymptotically stable*. In particular, constructive and explicit mathematical inequalities are given for identifying the region in the CNN parameter space where complex phenomena may emerge, as well as for localizing it further into a relatively small parameter domain called the edge of chaos (regions [5], [7], and [8] in Fig.9) where the potential for emergence is maximized.

*Consequently: he who wants to have right without wrong,  
Order without disorder,  
Does not understand the principles  
Of heaven and earth.  
He does not know how  
Things hang together.*

*Chuang Tzu*

## References

1. J. H. Holland, *Emergence : from chaos to order*, Reading, Mass.: Addison-Wesley, 1998.
2. I. Stewart, *Life's other secret : the new mathematics of the living world*, New York : John Wiley, 1998.
3. H. Haken, "Visions of Synergetics," Special Issue on *Visions of Nonlinear Science in the 21st Century, International Journal of Bifurcation and Chaos*, 7(1997), pp.1927-1951.
4. R. Badii and A. Politi, *Complexity : hierarchical structures and scaling in physics*, Cambridge ; New York : Cambridge University Press, 1997.
5. C. G. Langton(Ed.), *Artificial life : an overview*, Cambridge, Mass. : MIT Press, 1995.
6. P. Coveney and R. Highfield, *Frontiers of complexity : the search for order in a chaotic world*, New York : Fawcett Columbine, 1995.
7. M. Gell-Mann, *The quark and the jaguar : Adventures in the simple and the complex*, New York : W.H. Freeman, 1994.
8. F. Crick, *The astonishing hypothesis : the scientific search for the soul*, New

- York : Scribner ; New York : Maxwell Macmillan International, 1994.
9. K. Mainzer, *Thinking in complexity : the complex dynamics of matter, mind, and mankind*, Berlin ; New York : Springer-Verlag, 1994.
  10. M. Eigen, *Steps towards life : a perspective on evolution*, Oxford ; New York: Oxford University Press, 1992.
  11. M. M. Waldrop, *Complexity: the emerging science at the edge of order and chaos*, New York : Simon & Schuster, 1992.
  12. L. Nadel and D. L. Stein, *1990 lectures in complex systems : the proceedings of the 1990 Complex Systems Summer School*, v. 3. of series *Santa Fe Institute studies in the sciences of complexity. Lectures*, Redwood City, Calif. : Addison-Wesley, 1991.
  13. S. Forrest(Ed.), *Emergent computation : self-organizing, collective, and cooperative phenomena in natural and artificial computing networks*, Cambridge, Mass. : MIT Press, 1991.
  14. G. Nicolis and I. Prigogine, *Exploring complexity : an introduction*, New York : W.H. Freeman, 1989.
  15. D. L. Stein(Ed.), *Lectures in the sciences of complexity : the proceedings of the 1988 Complex Systems Summer School held June-July 1988 in Santa Fe, New Mexico*, Redwood City, Calif. : Addison-Wesley Pub. Co., Advanced Book Program, 1989.
  16. Paul Manneville, *Dissipative structures and weak turbulence*, Boston : Academic Press, 1990.
  17. R. Kapral and K. Showalter (Eds.), *Chemical waves and patterns*, v. 10 of series *Understanding chemical reactivity*, Dordrecht ; Boston : Kluwer Academic Publishers, 1995.
  18. D. Walgraef, *Spatio-temporal pattern formation : with examples from physics, chemistry, and materials science*, in series *Partially ordered systems*, New York : Springer, 1997.
  19. L.O. Chua, "Guest Editorial," *Special Issue on Nonlinear waves, patterns and spatio-temporal chaos, IEEE Trans. on Circuits and Systems-I*, **42**(1995), pp.557-558, Oct. 1995.
  20. L. O. Chua and Y. W. Sing, "A nonlinear lumped circuit model for Gunn Diodes," *Int. Journal of Circuit Theory and Applications*, **6**(1978), pp.375-408.
  21. A. V. Holden, "Nonlinear Science—the impact of biology," Special Issue on *Visions of Nonlinear Science in the 21st Century*, *International Journal of Bifurcation and Chaos*, **7**(1997), pp.2075-2104.
  22. L. O. Chua, *CNN: A Paradigm for Complexity*, Singapore : River Edge, N.J. : World Scientific, 1998.
  23. R. N. Madan(Ed.), *Chua's circuit: A paradigm for chaos*, Singapore : River Edge, N.J. : World Scientific, 1993.
  24. L.V. Kantorovich and V.I. Krylov, *Approximate methods of higher analysis*, New York, Interscience, 1964.
  25. L.M. Milne-Thomson, *The calculus of finite differences*, London: Macmillan, 1960.
  26. V. Perez-Munuzuri, V. Perez-Villar and L.O. Chua, "Propagation failure in lin-

- ear arrays of Chua's circuits," *International Journal of Bifurcation and Chaos in Applied Sciences and Engineering*, **2**(1992), pp.403-406.
27. C. Rovelli and L. Smolin, "Discreteness of area and volume in quantum gravity," *Nuclear Physics B*, **B442**(1995), pp.593-619.
  28. L.O. Chua and D.N. Green, "Graph-theoretic properties of dynamic nonlinear networks," *IEEE Trans. on Circuits and Systems*, **CAS-23**(1976), pp.292-312.
  29. L.O. Chua, "A qualitative analysis of the behavior of dynamic nonlinear networks: stability of autonomous networks," *IEEE Trans. on Circuits and Systems*, **CAS-23**(1976), pp.355-379.
  30. L.O. Chua, "Dynamic nonlinear networks: state-of-the-art," *IEEE Trans. on Circuits and Systems*, **CAS-27**(1976), pp.1059-1087.
  31. L.O. Chua, "Nonlinear circuits," *IEEE Trans. on Circuits and Systems*, **CAS-31**(1976), pp.69-87.
  32. L.O. Chua, M. Hasler, G.S. Moschytz, J. Neiryneck, "Autonomous cellular neural networks: a unified paradigm for pattern formation and active wave propagation," *IEEE Transactions on Circuits and Systems I: Fundamental Theory and Applications*, **42**(1995), pp.559-577.
  33. Brian D. O. Anderson and S. Vongpanitlerd, *Network analysis and synthesis: a modern systems theory approach*, in *Prentice-Hall electrical engineering series. Prentice-Hall networks series*, Englewood Cliffs, N.J., Prentice-Hall, 1973.
  34. R. Dogaru and L.O. Chua, "Edge of chaos and local activity domain of FitzHugh-Nagumo equation," *International Journal of Bifurcation and Chaos in Applied Sciences and Engineering*, **8**(1998), pp.211-257.
  35. R. Dogaru and L.O. Chua, "Edge of chaos and local activity domain of the Brusselator CNN," *International Journal of Bifurcation and Chaos in Applied Sciences and Engineering*, **8**(1998), pp.1107-1130.
  36. R. Dogaru and L.O. Chua, "Edge of chaos and local activity domain of the Gierer-Meinhardt CNN," *International Journal of Bifurcation and Chaos in Applied Sciences and Engineering*, **8**(1998), pp.2321-2340.
  37. L. Min, K.R. Crouse, and L.O. Chua, "Analytical criteria for local activity and applications to the Oregonator CNN," *International Journal of Bifurcation and Chaos in Applied Sciences and Engineering*, **10**(2000), in press.